

Variability of Radiatively Forced Diurnal Cycle of Intense Convection in the Tropical West Pacific

W. M. Gray, J. D. Sheaffer, and W. B. Thorson
Colorado State University
Fort Collins, Colorado

Introduction

Strong differences occur in daytime versus nighttime (DVN) net radiative cooling in clear versus cloudy areas of the tropical atmosphere. Daytime average cooling is approximately $-0.7^{\circ}\text{C}/\text{day}$, whereas nighttime net tropospheric cooling rates are about $-1.5^{\circ}\text{C}/\text{day}$, an approximately two-to-one difference (Gray and Jacobson 1977). The comparatively strong nocturnal cooling in clear areas gives rise to a diurnally varying vertical circulation and horizontal convergence cycle. Various manifestations of this cyclic process include the observed early morning heavy rainfall maxima over the tropical oceans. The radiatively driven DVN circulation appears to strongly modulate the resulting diurnal cycle of intense convection which creates the highest, coldest cloudiness over maritime tropical areas and is likely a fundamental mechanism governing both small and large scale dynamics over much of the tropical environment.

Data and Methods

Data include three-hour (i.e., eight images/day) satellite infrared (IR) and visible data for a total of 36 partly current months, extending from the mid 1980s through 1992. The satellite data are the International Satellite Cloud Climatology Project B-1 data, which have a 10-km radiance sampling interval. Periods of study emphasize the summer and winter months with, at this point, comparatively less analysis for the transition seasons. Depending on our purpose, data are expressed either as emittance values (Watts/m^2) or as Equivalent Blackbody Temperatures (EBTs).

Results

The map and analysis in Figure 1 show the distribution of EBT-based pixel temperatures colder than -55°C , expressed as the percent of total pixel counts in each of 160 five-degree (lat/lon) "bins." As the domain spans seven time zones, local time for the (00Z) data in Figure 1 ranges from 0600 in the west to 1200 in the eastern most areas.

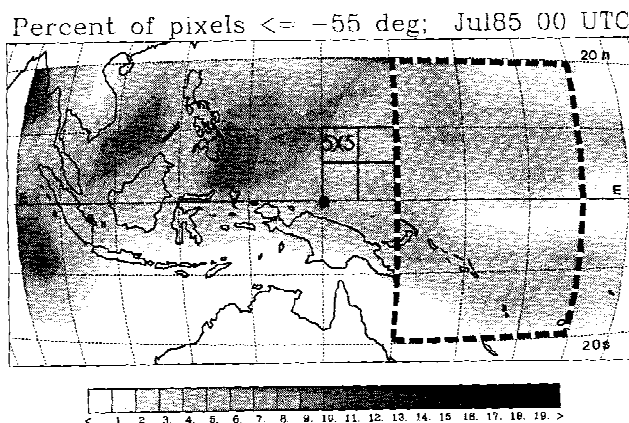


Figure 1. Map showing analysis domain for GMS OLR data. Basic spatial units are five by five latitude-longitude areas, four of which are shown outlined by solid lines in the area north of Papua New Guinea; the large dot on the equator at 140°E shows the approximate satellite sub-point and the large area outlined between 150°E to 180° , 20°N to 20°S is the subject of analyses in Figures 2 and 3. Shading shows areas of intense convection at 00Z during July 1985.

Retaining the data as "pixel counts" in the resolved B-1 mode for fairly narrow temperature bands offers greater accuracy for studying the diurnal cycle than does creating various time or space averaged values.

Observations include a comparatively sharp drop-off of pixel counts at temperatures below -45°C . This effect is roughly consistent with the prior observation of -45°C as the coldest IR temperature normally observed for residual thin stratus clouds. Another sharp drop of pixel counts occurs for temperatures colder than -65°C . Prior work suggests that the mixing ratios associated with maximum sea surface temperature values observed in the West Pacific warm pool correspond to latent heat release and buoyancy of undiluted convective parcels up to approximately 150 mb.

Hence, as the observed mean air temperature is about -65°C at 150 mb, the rapid decrease in the incidence of pixels colder -65°C is consistent with comparatively small areas of actively overshooting convective plumes at these -65°C temperatures.

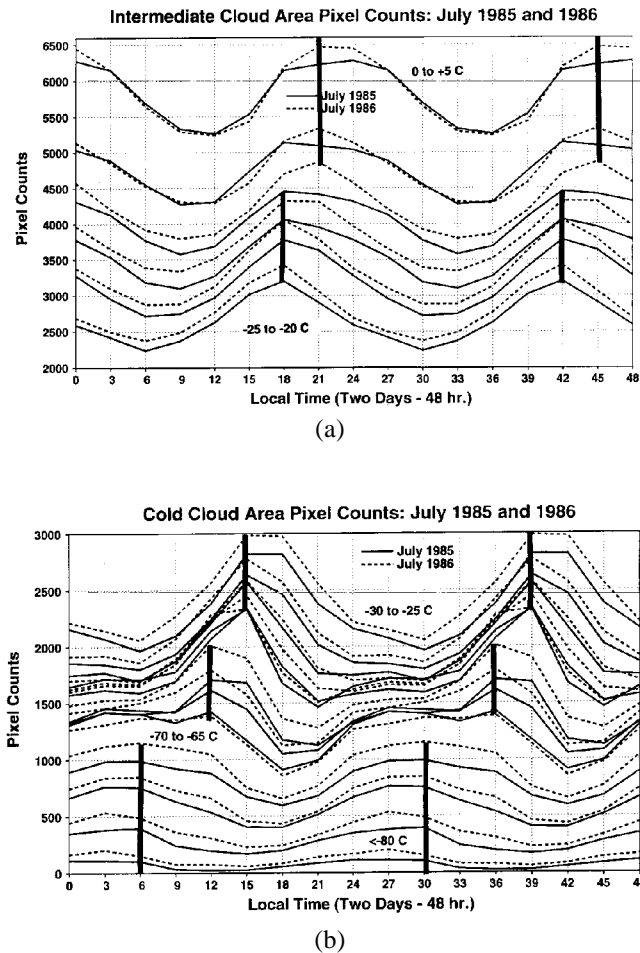


Figure 2. Diurnal variation of pixel counts for the large area enclosed by 20°N to 20°S , 150°E to 180° shown in Figure 1. For clarity, two full daily cycles (48 hours) are shown beginning at midnight local time. The 12 temperature ranges in the lower panel span five degree increments, beginning at -80°C to -85°C (bottom) and warming to -25°C to -30°C (top). The dashed lines are for July 1986 (El Niño) versus solid lines for July 1985 (La Niña). Top Panel: As in the lower panel but for seven intermediate temperature ranges extending from -20°C to -25°C (bottom) to 0°C to $+5^{\circ}\text{C}$ (top). The two sets of vertical bars highlight temperature regimes maximizing at 1800 and 2100, respectively.

The analyses in Figure 2 show the diurnal cycle of pixel counts for a total of eighteen five-degree ranges spanning temperatures from colder than -80°C , at the bottom of lower panel, through $+5^{\circ}\text{C}$, at the top of the upper panel. Figure 3 shows diurnal cycles of total outgoing longwave radiation (OLR) emittance for warm temperature ranges ($+5$ to $+30^{\circ}\text{C}$). Data for two years, 1985 and 1986, are included in Figure 2 to show the year-to-year consistency as well as differences linked to El Niño (1986). One thousand pixels correspond to about one percent of the large sub area in Figure 1; hence, all of the area colder than -65°C occupies only about 3% of the special area, whereas the emittance curve in Figure 3 represents about 70% of the area.

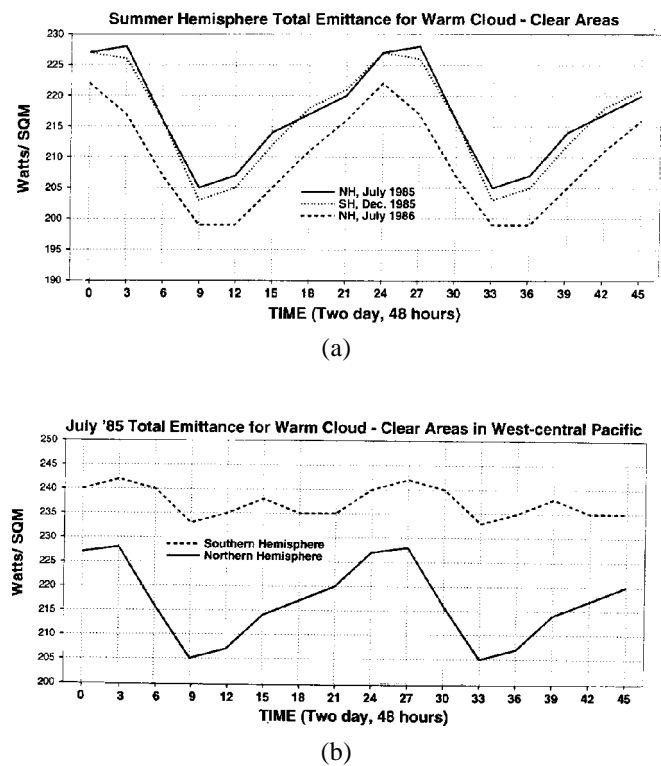


Figure 3. Comparative diurnal cycles of warm area ($+5$ to $+30^{\circ}\text{C}$) emittance for portions of the analysis area in Figure 1. Top panel shows cycles for July 1985 (La Niña), July 1986 (El Niño), and December 1985; data are for the summer hemisphere so that July plots are for $0-20^{\circ}\text{N}$, whereas December plots are for $0-20^{\circ}\text{S}$ (150E to DL). Bottom panel compares concurrent “summer” and “winter” hemisphere cycles for July 1985.

The very coldest clouds and most intense convection represented in Figure 2 reach their maxima around 0300 to 0600 local time, whereas somewhat warmer clouds associated with stratiform cirrus clouds (i.e., warmer than -65°C) initially increase in phase with the very coldest clouds but go on to achieve appreciably stronger maxima later in the day, in a 1200-1500 time frame. A distinct phase propagation of increased pixel incidence occurs starting from the coldest EBT values in the early morning through the -20 to 0°C temperature domains by the late afternoon. This trend is accentuated in Figure 2 by the sequence of vertical bars.

The total area of relatively clear conditions and warmer temperatures represented in Figure 3 ($\text{EBT} > +5^{\circ}\text{C}$) increases closely in phase with the intense ($< -65^{\circ}\text{C}$) convection, also reaching a morning maximum. The temporal concurrence of the maxima of coldest and warmest areas reflects the influence accelerating rates of subsidence in the “clear” areas manifest as increasingly larger areas of warm EBT; this trend begins at sunset and accelerates during the night, leading to maximum warm area extent in the late morning hours.

Discussion

The diurnal march of interactive clear versus cloudy area radiative forcing of the nocturnal maximum of intense tropical convection can be inferred directly from Figures 2 and 3. As seen in the warm area emittance cycles (Figure 3), net heat loss begins increasing at sunset (1800) and accelerates throughout the night. The associated broad scale subsidence in these areas immediately begins to enhance low level convergence into the smaller intervening cloudy areas wherein convection intensifies, creating the observed late night-early morning maximum of very cold EBT values.

During daylight hours this forcing subsides, and the morning maximum of very cold EBT systematically gives way to warmer intermediate values (-55 to -20°C) associated largely with stratiform cloud, which spreads rapidly in late morning to a maximum in late afternoon—after which the cycle begins again. This same sequence is seen to play out over the entire maritime portion of the Tropical West Pacific with only modest seasonal differences in component amplitudes. El Niño-Southern Oscillation-linked differences reflect east-west adjustments of the convective centers, but with the same late night/early morning maximum of intense convection. Future research entails expanding these analyses to include detailed validation and quantification of our observations in the Tropical Ocean Global Atmosphere Coupled Ocean Atmosphere Response Experiment data including microwave data, soundings, and regional precipitation analyses.

Acknowledgments

This research is sponsored by the Environmental Science Division of the Department of Energy, Grant No. DE-F603-94-ER61772 as part of the Atmospheric Radiation Measurement Program. Barbara Brumit and Amie Hedstrom provided assistance in manuscript preparation. Profiler data were provided by Ken Gage, with timely assistance from Tony Riddle.

Reference

Gray, W. M., and R. Jacobson, Jr. 1977. Diurnal variation of deep cumulus convection, *Mon. Wea. Rev.*, **105**, 1171-1188.